Merging criteria for the definition of a local pore and the CSD computation of granular materials

F. Seblany
[1]Université de Lyon, Ecole centrale de Lyon, LTDS, UMR CNRS 5513, 36 av Guy de Collongue 69134 ECULLY CEDEX, France

U. Homberg[2], E. Vincens[1], P. Winkler[3] & K.J. Witt[3]
[2]Zuse Institute Berlin, Department Visual Data Analysis, Takustr. 7, 14195 Berlin-Dahlem, Germany
[3]Bauhaus-Universität Weimar, Chair of Geotechnical Engineering, Coudraystrasse 11c, 99421 Weimar, Germany

Abstract: Granular filters are materials used to avoid mass transport under seepage flow. They are installed in zoned dams or on the downstream slope of levees to prevent the wash out of soil particles through the core of the earth structures or through its foundation. This migration is stopped if the particles are blocked on their pathway by a constriction smaller than their own size. In that sense, the constriction size distribution is closely related to the filtering capability of the granular filter. Different numerical methods exist to study and divide the pore space into local pores and then constrictions. However, they all require a statement of what a local pore is. Al-Raoush et al. (2003) noticed that the partition of the void space may lead to an over-segmentation of the pore space and merging criteria may be used to define more physical local pores. Conversely, merging may require thresholds that may influence the final degree of the segmentation. In this paper, we compare different merging criteria and discuss their implication on both the local pore definition and the constriction sizes statistical distribution. Moreover, since the constriction size distribution is often used in probabilistic approaches for filtration, we insist on the necessary consistency of the choice of a given merging criterion with other possible statements related to these probabilistic approaches.

Keywords: constriction, sphere packing, probabilistic approach, filtration

1 INTRODUCTION

Internal erosion is one of the leading causes of failure of earth structures used in hydraulic engineering and for flood protection (earth dams, levees). This phenomenon occurs when fine particles are detached and transported through the porous medium due to a seepage flow. Granular filters are installed during the construction works in hydraulic structures or on their downstream slopes when repairing in order to avoid or to limit the migration of fine particles. In such a circumstance, they are supposed to mitigate internal erosion.

A granular medium includes a set of connected pores between solid particles that form a continuous network through which a fluid can flow. The constrictions are the narrowest sections linking larger volumes (pores) and are statistically described by means of a cumulative constriction size distribution (CSD).

The retention capacity of a granular filter is mainly related to the geometrical characteristics of its void space. More precisely, the performance of a granular filter can be evaluated and characterized using the information provided by the CSD. Indeed, based on the probabilistic concepts of Silveira (1965), the CSD is related to the probability for a fine particle of diameter d to cross a constriction having the same size. In fact, fine particles smaller than the smallest constriction d_{Cmin} can cross the entire filter

(probability of passing = 1). Conversely, all particles larger than the largest constriction d_{Cmax} will not enter the filter (probability of passing = 0) (Fig. 1.1).

There are different ways to obtain the CSD: experiments (Witt, 1986; Soria et al., 1993), analytical approaches (Locke et al., 2001; Reboul et al., 2010) and numerical approaches (Reboul et al., 2008; Homberg et al., 2012; O'Sullivan et al. 2015).

To overcome some limitations associated with experimental methods, a powerful numerical tool, the Discrete Element Method (DEM), can be used to study modelled granular materials such as packings of spheres and to numerically generate them. The pore space of such packings can be extracted by combining the DEM with spatial partitioning techniques: the Delaunay tessellation or its dual, the Voronoi algorithm. In the Delaunay tessellation, the primary definition for a local pore is the Delaunay cell, i.e., a tetrahedron. The associated void volume can then be deduced for example by computing the largest void sphere inscribed between the four particle vertices of the tetrahedron. Constrictions are found on the four faces of each tetrahedron and are defined as the largest empty discs that can be inscribed between the three particle vertices of a tetrahedron face (Fig. 1.2) (Al-Raoush et al., 2003; Reboul et al., 2008). Obviously, the derived partition of the void space is artificial and a Delaunay cell is merely related to the underlying mathematical process of finding the three closest neighbors of a given particle to generate a tetrahedron. The computation of pores and constrictions are feasible for a granular material made of spheres but is very difficult to handle in the case of irregularly shaped particles.

To solve this issue, Homberg et al. (2012) have developed a voxel-based approach that computes a Voronoi-like decomposition based on a distance mapping on the pore space and the particle regions and extracts the median paths of the void space. Along these paths, the center of pores, the pore diameters and the local minima associated to constriction sizes can be determined.

One of the obstacles related to these methods is to identify pore structures that may hold a physical meaning. In this context, Al-Raoush et al. (2003) were using a Delaunay tessellation and found that the inscribed void sphere confined in each tetrahedron is not necessarily entirely included inside that tetrahedron, and two inscribed void spheres from two neighboring tetrahedra may overlap. According to these authors, it signifies that the opening size between two adjacent tetrahedra may be high enough to indicate a strong interconnection between them which is reflected by this overlapping. As a result, the tetrahedral tessellation would tend to abusively subdivide a complete pore structure into zones.

For the same reason, Homberg et al. (2012) considered that a merge between two adjacent pores may be required when the constriction size linking these pores is very close to that of the smallest pore. In fact, in such a case, pores are interconnected and seem to belong to a single entity. Figure 1.1(b) illustrates such a case where two adjacent pores (hatched and shaded area) are going to be merged.

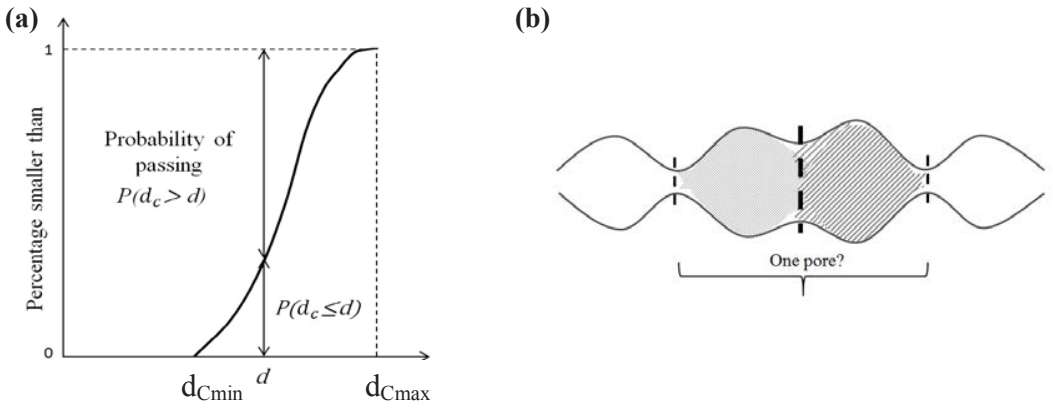

Figure 1.1. **(a):** Constriction size distribution and probability for a fine particle of diameter *d* to pass a constriction of its own size; **(b):** Scheme of a typical case encountered during pore merging.

Because different methods may lead to different pore structures and as a consequence to a different set of constriction sizes, this study aims to understand better the implications of using a given merging criterion on the pore and constriction statistics. Conversely, this paper does not address the definition of what a physical local pore should be since no clear definition for a local pore can be stated. In a second part, the impact of the merging criteria on the estimate of the average unit path distance (average distance between consecutive throats through the granular filter) is addressed.

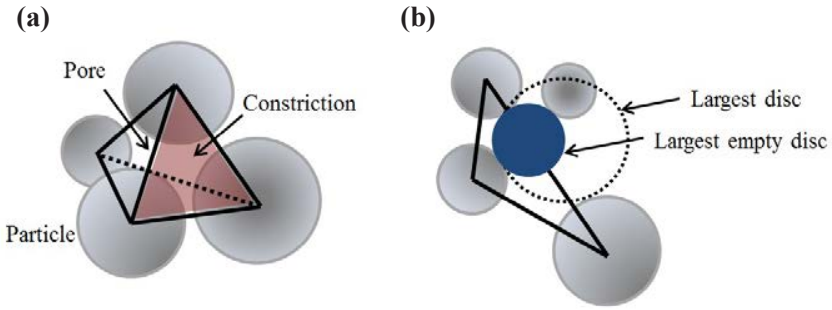

Figure 1.2. **(a):** Tetrahedron built from the centers of four neighboring spheres; **(b):** Definition of a constriction: the largest disc included in the void space for a given face.

2 GENERATION OF NUMERICAL SAMPLES

The open-source code Yade-DEM (Smilauer et al., 2010) was used to generate the numerical samples. The grading of the material is given in Figure 2.1 and is merely the one used in a previous study (Vincens et al., 2015). The minimum and maximum diameters D_0 and D_{100} for this material are respectively equal to 3 and 12 mm, and the coefficient of uniformity is equal to 1.7. Particles are represented by spheres that can move according to Newton's laws. The interaction between particles are governed by elastic-frictional contact forces with normal and tangential stiffness (K_n and K_t) and Coulomb friction angle (φ). A sample composed of 630 particles is created by isotropic compression which produces a homogeneous sample in terms of porosity and CSD. Periodic boundary conditions are used to eliminate the wall effect, which disturbs the self-order of the spheres. Two samples are generated, one corresponding to the loosest state (UGL) and another one for the densest state (UGD) for the uniformly graded material. The coefficient for inter-particles friction is initially set to 0.7 and then decreased to reach the desired porosity (0.38), i.e., the porosity obtained by experiments on similar materials for the loosest state (Biarez and Hicher, 1994). The densest state, with a porosity of 0.34, is obtained by setting the friction value at contact to zero and allowing the system to equilibrate.

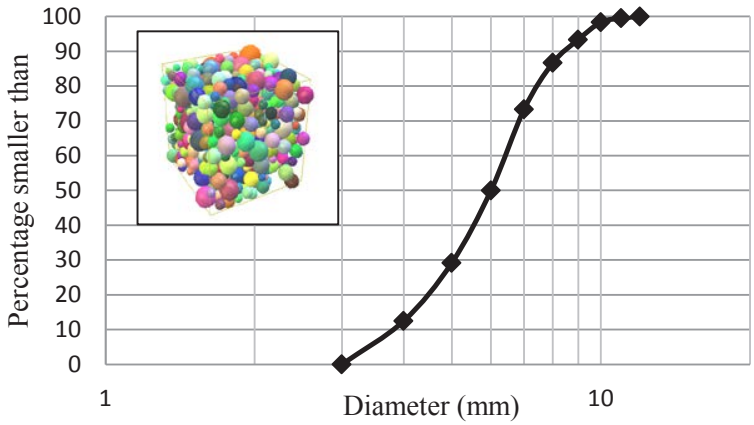

Figure 2.1. Particle size distribution for the studied material (the numerical sphere packing corresponds to the UGL material).

3 OVERLAPPING INSCRIBED VOID SPHERES APPROACH

Once the locations and radii of the spherical particles are known, a modified (weighted) tetrahedral tessellation is performed. The space is then partitioned into tetrahedra with vertices on the center of neighborhood spheres.

Such a 3D tessellation provides an essential step for spatial analysis of the packing. Thus, each tetrahedron represents a local pore (which volume is estimated by the largest inscribed void sphere) and four throats (the largest empty discs on tetrahedron faces). They are obtained using optimization algorithms; more details can be found in Al-Raoush et al. (2003) and Reboul et al. (2010). The resultant CSD corresponds to level 0 (L_0) by Reboul et al. (2008).

However, the direct computation from Delaunay tessellation includes configurations where constrictions are larger than pores (constrictions formed by non-touching particles) and other configurations where two adjacent inscribed void spheres are superimposed. Such cases correspond to tetrahedra of undesirable shape (e.g., flat tetrahedra). Level L_0' guarantees the removal of these degenerated constrictions.

As mentioned before, two adjacent inscribed spheres may overlap and then should be distinguished from those which are completely separated. Different merging criteria of pores are then defined as shown in Figure 3.1.

Level 1-p% (L_1-p%) is a user controlled merging step applied when two adjacent inscribed void spheres with diameters d_{Pi} and d_{Pj} overlap each other and are connected by a constriction C_{ij} with a diameter $d_{Cij} \geq (p/100) \times min(d_{Pi}, d_{Pj})$, p being a given percentage. For Level 1 (L_1), the overlap of the inscribed void spheres is the only condition required to merge adjacent pores.

A further level of merging is studied (Level 2b (L_{2b}) and Level 2 (L_2)) where the merging criterion is not only applied to the adjacent local pore but also to the next adjacent local pore. A restriction of L_2 is introduced and is denoted L_{2b} where the inscribed void spheres must be arranged in decreasing orders to induce a merging. This criterion takes into account the geometric constraints to define the pore entity. Indeed, the transition between pores is characterized by constricted regions followed by more expanded regions.

It should be noted here that after merging two neighboring pores (three neighboring pores in case of L_{2b} and L_2), the interconnection between the newly formed pore with its neighboring pores is not checked, since an extra level of merging tends to create ducts within the granular medium.

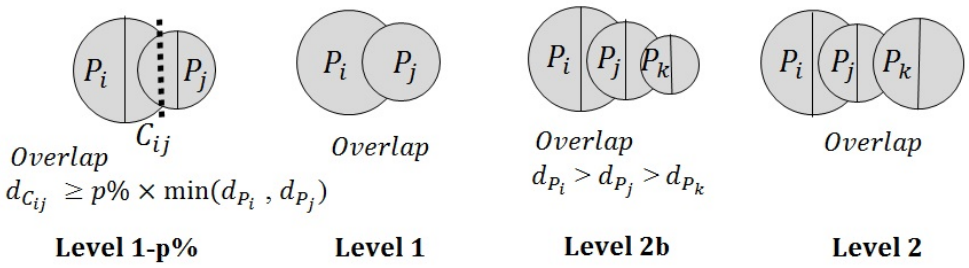

Figure 3.1. Definitions of different merging criteria based on the overlapping of inscribed spheres associated to adjacent pores.

4 HIERARCHICAL MERGE

The hierarchical merge method requires a graph data structure representing the pore network. For this study, the graph is obtained from a voxel-based approach (Homberg et al., 2012) that represents the medial paths of a distance mapping of the pore space to the surrounding particles. The graph vertices are located at local maxima and are assumed to represent pore centers, while the edges represent the pore paths running along the maximal distances between two adjacent pores centers. The distance information is tracked along the edges, where the constriction is defined as the point having the smallest distance

along an edge (Fig. 4.1(a-b)). To extract the graph from the studied samples, the sphere packings were scan-converted into voxel data sets with a voxel size of 0.02 × 0.02 × 0.02 mm^3 (0.02 mm= $D_0/150$). The discrete nature of the voxelization and the Voronoi-typical degenerated cases produce additional pore centers and constrictions in the graph that do not correspond to real maxima. Such cases have no diameter differences between constriction and smaller pore and will be merged at the beginning of the hierarchical merge, which then corresponds to the result of L_0'.
This hierarchical method evaluates the separation of a pair of pores P_i and P_j by their constriction C_{ij} based on the relative diameter difference $t_{diff}(P_i, C_{ij}, P_j) = (d_P - d_{Cij})/d_P$ with $d_P = min(d_{Pi}, d_{Pj})$ and $i \neq j$. The value t_{diff} will be used to build hierarchical neighbors of pores according to their degree of separation, which is specified by a user-defined threshold t. *Note*, t corresponds to p with t=1-p/100, the threshold introduced in L_1-p%. This approach was developed for materials with irregular particles and does not consider sphere overlaps in order to include pairs within elongated pores.

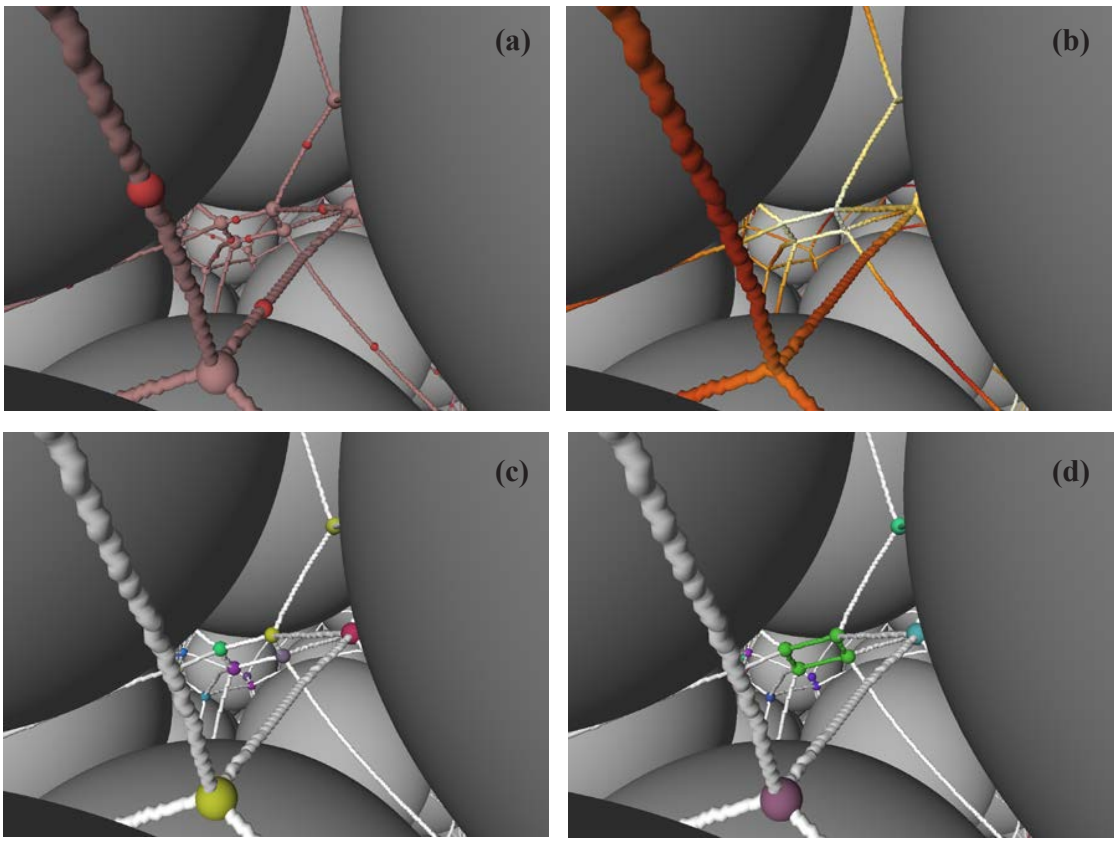

Figure 4.1. Detail of spheres and graph extracted from the voxelization of the UDG material. For visibility, the radius of the particle spheres was reduced to 90%. **(a):** Larger spheres at crossings indicate pore centers; smaller, darker spheres indicate constrictions. **(b):** The diameter is attached to each edge point and color-coded with yellow (large) to red (small). **(c):** Unmerged pore centers are randomly colored by their label id. **(d):** Merged pore centers and their connection paths and constrictions will be labeled as belonging together (*t=1%*).

The hierarchical manner arises from specifying tuples $T_{ij} = (P_i, C_{ij}, P_j, t_{diff}(P_i, C_{ij}, P_j))$ of two pores, their constriction and the difference threshold t_{diff} and from the order of processing them. The approach starts from tuples of direct neighbors in the unmerged graph (Fig. 4.1(c)) and evaluates them in increasing order of the difference thresholds. Each step assigns the smaller pore and its constriction to the larger pore. The neighbor tuples that contain the merged pore will be updated by replacing the smaller pore by the larger one as well as by re-computing t_{diff} accordingly. For example, if $d_{Pi} < d_{Pj}$, then all neighbor tuples T_{ik} with $k \neq j$ will be converted to $T_{jk} = (P_j, C_{jk}, P_k, t_{diff}(P_j, C_{jk}, P_k))$ to be neighbors of P_j. P_i and C_{ij} are labeled on the graph as belonging to P_j (Fig. 4.1(d)) and will be discarded from further

considerations. This is then repeated until all (newly created) tuples that have a difference threshold $t_{diff} \leq t$ are processed. More algorithmic details can be found in Homberg et al. (2014).

The remaining tuples represent hierarchical neighbors rather than direct neighbors where each pore represents all hierarchically assigned pore centers. The constriction and t_{diff} represent the most significant separation between the two representative pores, which increase their life time as separated pores compared to the direct neighbor relations and avoids an inappropriate merge propagation.

5 RESULTS AND DISCUSSION

The initial CSDs (L_0) derived from the Delaunay and the voxel-based methods are almost congruent for a sufficient small voxel size (Vincens et al., 2015). For convenience, we only present in the following the results corresponding to the UGL material, but similar results were found for the UGD material. The evolution of the number of constrictions (normalized to the initial total constrictions in the sample before merging) corresponding to different criteria is presented in Figure 5.1. Then, Figure 5.2 and Figure 5.3 show the CSDs and the estimated probability density of constriction sizes for different merging criteria described in sections 3 and 4 respectively. It should be noted that the CSD corresponding to L_0' is located between the CSDs associated to L_0 and L_1-99% and is not shown in Figure 5.1.

First, one can note that merge involving overlapping adjacent inscribed spheres (Fig. 5.1(a)) tends to limit the possibility for merging contrary to the hierarchical merge (Fig. 5.1(b)), which guaranties that no pore structure such as ducts would be identified. Any less restrictive criterion than L_1-90% does not provide further merging and the resulting pore structure is similar to that provided by L_1 merging which means that such cases are generally not present in the packing of spheres. Moreover, L_2 merging just provides few further merged pores than L_1.

Another feature is observed in Figure 5.2(b) and Figure 5.3(b). Merging tends to let appear a clear and single mode while vanishing a coupled second higher mode. When merging, the first mode for the constriction size almost stabilizes irrespective of the kind of level (Level 1-p%, Level 1 or Level 2) or the threshold value t in the hierarchical approach if this latter one remains smaller than 10% (not shown herein). If the threshold value t is too high, for example 30% in Figure 5.3(a), one can note that the CSD shifts towards the smallest diameters. In this case, it implies that the deduced pore structure is changing of kind.

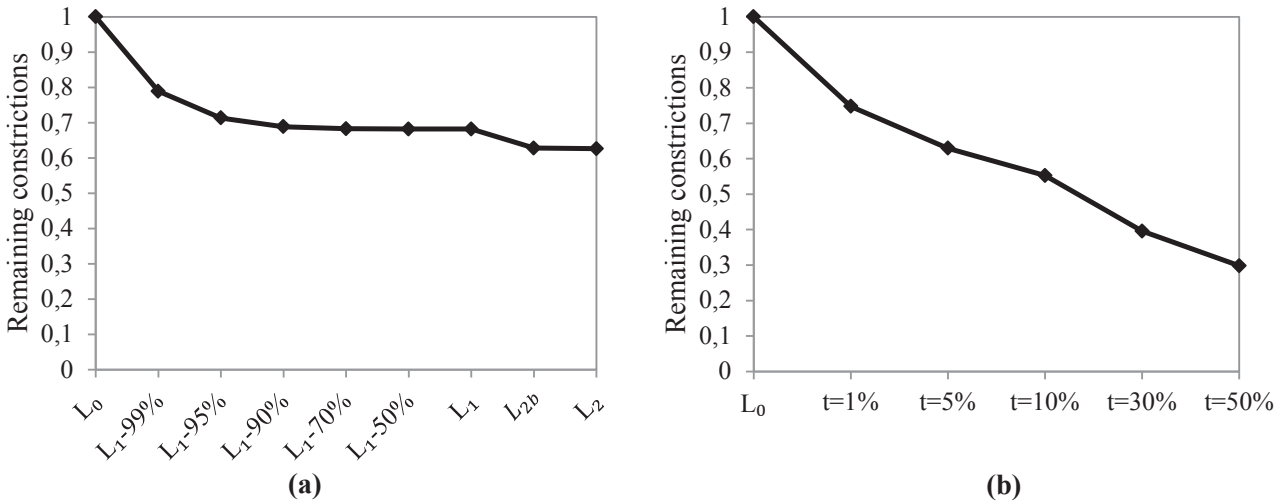

Figure 5.1. Evolution of the relative number of constrictions for different merging criteria. **(a):** merge associated to overlapping inscribed void spheres; **(b):** Hierarchical merge.

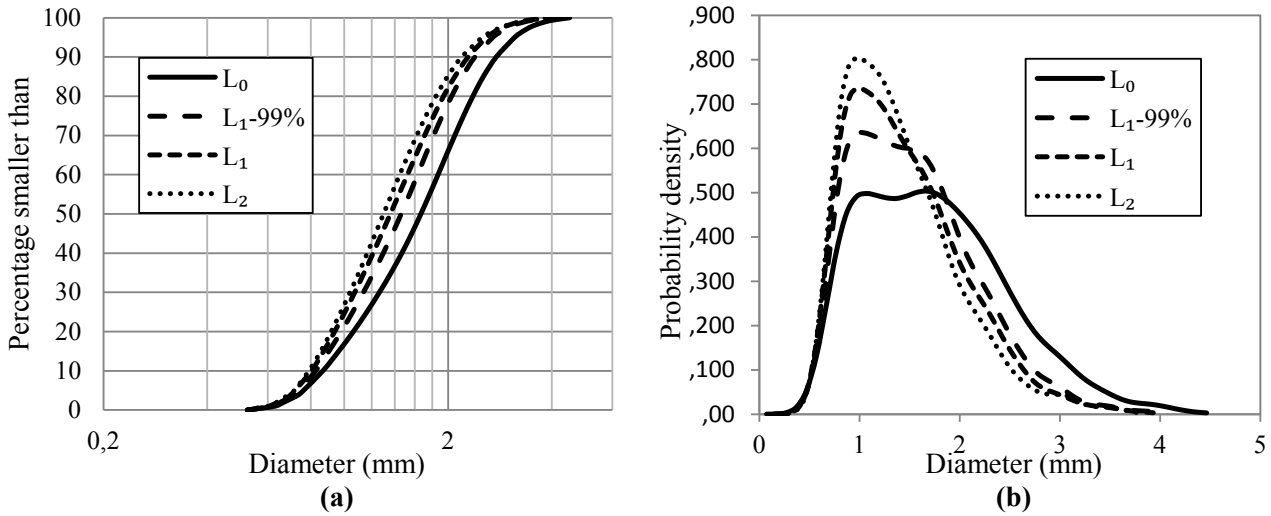

Figure 5.2. **(a):** CSDs for the UGL material; **(b):** underlying probability density function for different merging criteria defined in the overlapping inscribed void spheres approach.

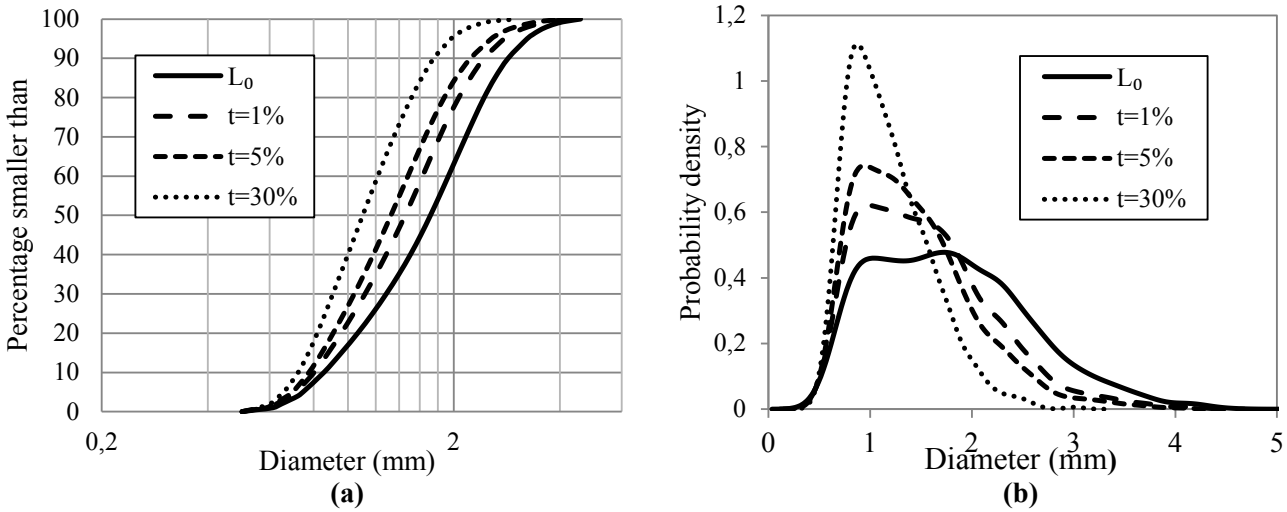

Figure 5.3. **(a):** CSDs for the UGL material; **(b):** underlying probability density function of the constriction diameter for different steps of hierarchical merge.

When analyzing in more detail the different approaches for merging, first, the L_1-p% considers two local properties to evaluate the constrictions: the overlap between adjacent pores and the comparison of the size of constriction connecting two pores to the size of the smallest one, while the hierarchical approach evaluates the degree of separation between pores in a global scope, independently of overlaps. The combination of the overlap and the constriction criterion imply a criterion based on the distance between pores which seems to be more reasonable according to Al-Raoush et al. (2003) where neighboring pores are merged if the center of a void inscribed sphere lies within the adjacent inscribed sphere. In fact, a statistical study over all tuples (P_i, C, P_j) shows that both properties are verified when p=99-95% (t=1%-5% in hierarchical merging). By decreasing the merging threshold p, more constrictions linking non-overlapping pores are found. In this case, the number of deleted constrictions increases dramatically in the hierarchical merge. That is to say that the comparison between the two merging methods should be restricted to the smallest thresholds (t=1%-5%).

Furthermore, one should expect that more constrictions can be removed in the hierarchical merge steps, since it allows merging multiple pairs as long as the newly created neighbors also meet the specified difference threshold, in contrast to L_1-p% where the merging criterion is only applied to the

first neighbor as explained in sections 3 and 4. Figure 5.4 shows that the CSD derived from L_1-99% and that corresponding to t=1% are approximately similar while the CSD (t=5%) is closer to that of L_2.

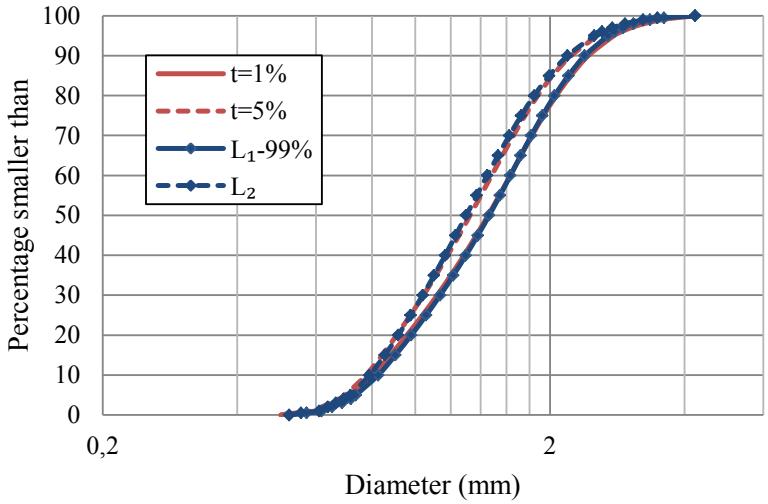

Figure 5.4. Comparison of the CSDs resulting from different merging processes.

After comparing different merging criteria and their associated CSDs, it is important to study how the choice of a certain criterion impacts the processing of the filtration probabilistic theory which assigns the coordinate of the CSD curve to the capture probability of a fine particle by a constriction of its own size.

In the framework of the filtration theory proposed by Silveira (1965), filter constriction sizes are related to the possibility for the transport of base particles of a given diameter. Stating that the pore network is organized according to a regular cubic model forming unit layers (Schuler, 1996) and that the displacement of particles is mainly unidirectional, the probability of passing one unit layer P_u is equal to that of passing one constriction P. P' is the probability to be stopped after a path corresponding to n layers. The total distance covered by a fine particle having diameter d is given by Equation (1).

$$L = n \times s = log\ (1 - P') \times s / log\ P_u \quad (1)$$

where s is in that case the average distance between two confrontations, which is also the average unit layer thickness. The estimate of s is a challenging problem and different proposals are found in the literature: D_{50} by mass (Soria et al., 1993), D_{50} by number (Locke et al., 2001), D_{50} by surface area (Indraratna et al., 2007) or the mean pore inscribed sphere computed from the Delaunay method (Sjah et al., 2013). In fact, there is little evidence so far for the choice of one between these options.

A quick estimate of the average thickness of a unit layer s can be given by the mean distance between centers of adjacent pores computed from the initial statistics over the entire sample (non-directional approach using either overlapping inscribed void spheres approach or the hierarchical method). When applying the merging criteria, the number of constrictions is reduced and then the value of s tends to increase. In other words, each merging criterion must be associated with a corresponding average unit layer. The results of this calculation are given in the second column of Table 1 and Table 2 for merging criteria associated to the overlapping inscribed void spheres approach and hierarchical approach respectively.

It should be noted that the estimated s corresponding to L_0 for the different merging processes are slightly different (s=2 mm in Tab 1. and s=1.7 mm in Tab 2.). This is can be justified by the fact that the CSDs resulting from L_0 using a Delaunay tessellation or a voxelization plus a distance mapping approach are not strictly identical. Moreover, the use of a specified merging criterion may lead to a s value that is greater than the reference s value found for L_0 by an amount of 90%, which is significant.

On the other hand, the maximum path length L_{max} for a particle of a given diameter d (e.g., 1.16mm herein), using Equation (1) was computed. We consider a confidence level of P'=95% (Locke et al.,

2001) and P (equal to P_u if a unidirectional pathway is stated) is obtained directly from the CSDs associated to different merging criteria (Fig. 1.1(a)). Thus, for the different merging criteria mentioned in Table 1, P is equal to 0.75, 0.69, 0.65 and 0.62 for L_0, L_1-99%, L_1 and L_2 respectively. In Table 2, P corresponds to 0.76, 0.69, 0.64 and 0.59 for L_0, t=1%, t=5% and t=10% respectively.

A consistent method would imply to use the s value corresponding to a merging criterion to compute L_{max}, which is not generally the case in the literature. In Table 1 and Table 2, one can note that if a consistent value for s is used, the maximum length L_{max} computed by the probabilistic approach is rather stable (around 21 mm for merging criteria associated to the overlapping inscribed void spheres approach (see diagonal line in Tab. 1) and 19 mm for the hierarchical merging method (see diagonal line in Tab. 2)).

On the contrary, L_{max} is considerably underestimated (L_{max}= 12.8 mm) if P value corresponding to L_2 (P=0.62) is combined with s value estimated from L_0 (s=2 mm) in Equation (1). The same holds true in the case of the hierarchical method. If the s value (s=1.7 mm) for L_0 is used together with a CSD computed with a merging threshold t=10%, the error made for the estimate of L_{max} approximates 45%.

Table 1. The longest distance L_{max} traversed by a particle of diameter d=1.16 mm for the merging criteria associated with the overlapping inscribed void spheres approach.

Merging criterion		L_{max} (mm)			
		L_0	L_1-99%	L_1	L_2
L_0	s=2.0 mm	21.2	16.5	14.2	12.8
L_1-99%	s=2.6 mm		21.0	18.1	16.3
L_1	s=3.0 mm			20.9	18.8
L_2	s=3.3 mm				20.4

Table 2. The longest distance L_{max} traversed by a particle of diameter d=1.16 mm for the hierarchical merging approach.

Merging criterion		L_{max} (mm)			
		L_0	t=1%	t=5%	t=10%
L_0	s=1.7 mm	19.0	13.5	11.7	9.9
t=1%	s=2.3 mm		18.8	15.6	13.2
t=5%	s=2.8 mm			18.6	15.7
t=10%	s=3.2 mm				17.9

6 CONCLUSION

Two techniques for computing the void characteristics of sphere packings (pore and constriction sizes) are compared. Both methods provide the same initial CSD. Different merging criteria can be adopted to associate the interconnected local pores, and consequently different final CSDs can be prescribed. Since there is no clear definition for a local pore, no definite criterion can be prescribed. Nevertheless, one can note that if a L_1 level criterion or a threshold value t equal or smaller than 1% (hierarchical merge) is chosen, the resulting CSD will be similar and the first mode of the probability density function that tends to emerge due to the merging process is not modified. Such criteria are recommended to define the average opening size of the filter from the CSD often associated to this mode.

In the other hand, if one needs to estimate, in the light of the probabilistic theory, the distance traveled by a fine particle through the filter, based on the CSD, attention must be paid to the choice of a consistent spacing between constrictions. The preliminary results have shown that the CSD and s must be concertedly and properly chosen, otherwise, the probabilistic method leads to significant errors for the estimate of the maximum travelled distance L_{max}.

ACKNOWLEDGEMENTS

Part of this work belongs to a project funded by *Compagnie Nationale du Rhône* (CNR). F. Seblany and E. Vincens acknowledge CNR for its interest and its financial support.

REFERENCES

Al-Raoush, R., Thompson, K., and Willson, C.S. (2003). Comparison of network generation techniques for unconsolidated porous media. *Soil Science Society of America Journal*, 67(6):1687–1700

Biarez, J., and Hicher, P.Y. (1994). *Elementary mechanics of soil Behavior, Classification of and correlations between parameters*. A.A. Balkema: Rotterdam, 81–106

Homberg, U., Baum, D., Prohaska, S., Kalbe, U. and Witt, K.J. (2012). Automatic Extraction and Analysis of Realistic Pore Structures from µCT Data for Pore Space Characterization of Graded Soil. *Proceedings of the 6th International Conference Scour and Erosion (ICSE-6)*, 66–73

Homberg, U., Baum, D., Wiebel, A., Prohaska, S. and Hege, H.C. (2014). Definition, Extraction, and Validation of Pore Structures in Porous Materials. *Topological Methods in Data Analysis and Visualization III*, Springer, 235–248

Indraratna, B., Raut, A.K. and Khabbaz, H. (2007). Constriction-based retention criterion for granular filter design. *Journal of Geotechnical and Geoenvironmental Engineering*, 133(3): 266–276

Locke, M., Indraratna, B. and Adikari, G. (2001). Time-dependent particle transport through granular filters. *Journal of geotechnical and geoenvironmental engineering*, 127(6):521–529

O'Sullivan, C., Bluthé, J., Sejpar, K., Shire, T. and Cheung, L. Y. G. (2015). Contact based void partitioning to assess filtration properties in DEM simulations. *Computers and Geotechnics*, 64, 120–131

Reboul, N., Vincens, E. and Cambou, B. (2008). A statistical analysis of void size distribution in a simulated narrowly graded packing of spheres. *Granular Matter*, 10(6):457–468

Reboul, N., Vincens, E. and Cambou, B. (2010). A computational procedure to assess the distribution of constriction sizes for an assembly of spheres. *Computers and Geotechnics*, 37(1):195–206

Silveira, A. (1965). An analysis of the problem of washing through in protective filters. *Proceedings of the 6th International Conference on Soil Mechanics and Foundation Engineering, Montréal, Que*, 551–555

Sjah, J. and Vincens, E. (2013). Determination of the constriction size distribution of granular filters by filtration tests. *International Journal for Numerical and Analytical Methods in Geomechanics*, 37(10):1231–1246

Šmilauer, V., Catalano, E., Chareyre, B., Dorofeenko, S., Duriez, J., Gladky, A., Kozicki, J., Modenese, C., Scholtès, L., Sibille, L., Stránský, J. and Thoeni, K. (2010). Yade Reference Documentation. In Yade Documentation (V. Šmilauer, ed.).

Soria, M., Aramaki, R. and Viviani, E. (1993). Experimental determination of void size curves. *Filters in geotechnical and hydraulic engineering*, 43–48

Vincens E., Witt K.J., Homberg U. (2015) Approaches to determine the Constriction Size Distribution for understanding filtration phenomena in granular materials, *Acta Geotechnica*, 10(3):291–303

Witt, K.J. (1986). *Filtrationsverhalten und Bemessung von Erdstoff-Filtern*, volume 104. Institut für Bodenmechanik und Felsmechanik der Universität Fridericiana in Karlsruhe.